ARTICLE

Chinese Journal of Structural Chemistry

P-Ni_4Mo Catalyst for Seawater Electrolysis with High Current Density and Durability

Gai Li[1], Suyang Feng[2], Jing Li[2]*, Peilin Deng[2], Xinlong Tian[2], Chongtai Wang[1] and Yingjie Hua[1]*

[1]*Key Laboratory of Electrochemical Energy Storage and Energy Conversion of Hainan Province, Key Laboratory of Electrochemical Energy Storage and Light Energy Conversion Materials of Haikou City, School of Chemistry and Chemical Engineering, Hainan Normal University, Haikou 571158, China*
[2]*State Key Laboratory of Marine Resource Utilization in South China Sea, Hainan Provincial Key Lab of Fine Chemistry, School of Chemical Engineering and Technology, Hainan University, Haikou 570228, China*

ABSTRACT Rational design of highly efficient and durable electrocatalysts with low cost to replace noble-metal based catalysts for seawater electrolysis is extremely desirable, but challenging. In this work, we demonstrate a rapid electrodeposition method by growing P-Ni_4Mo on the surface of the copper foam (CF) substrate to synthesize an efficient seawater electrolysis catalyst (P-Ni_4Mo/CF). The catalyst exhibited considerable HER performance and stability in alkaline seawater, with the overpotential as low as 260 mV at a current density of 100 mA cm^{-2}. The P-Ni_4Mo/CF is capable of achieving 1.0 A cm^{-2} with an overpotential of 551 mV, which is slightly worse than that of the Pt/C catalyst (453 mV). Moreover, P-Ni_4Mo/CF demonstrates robust durability, with almost no activity loss after the durability test for more than 200 h. This work not only reports a new catalyst for seawater electrolysis, but also presents a strategy for the performance enhancement of seawater electrolysis.

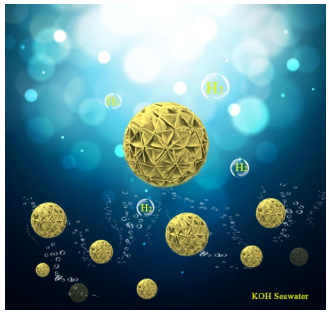

Keywords: seawater electrolysis, electrodeposition, hydrogen evolution reaction, phosphorus doping

n INTRODUCTION

Electrochemical water decomposition is one of the most attractive and sustainable technologies for the production of hydrogen by converting electrical energy into chemical energy.[1-6] The water electrolysis is carried out through the oxygen evolution reaction at the anode to produce oxygen and the hydrogen evolution reaction (HER) at the cathode to produce hydrogen.[7-11] HER is limited by the high price and stability of noble metal materials (Pt-based for HER), making them difficult to apply commercially on a large scale.[12,13]

Nowadays, non-noble metal electrocatalysts with high activity and long-term stability for electrocatalytic hydrolysis have been intensively investigated, and big achievements have been made.[14-17] On the other hand, it is well known that 96.5% of the global water resources is seawater, and freshwater resources are only about 1%,[18] while little has been done on the seawater electrolysis due to the main challenge of the chlorine evolution reaction, leading to the corrosion and fast performance decay of the catalysts. Therefore, the exploration of seawater electrolysis catalysts with low cost, resistance to seawater corrosion, and excellent stability is desirable option to promote the commercialization of related fields.[19,20] The application of some non-noble metal catalysts to the seawater electrolysis has been studied, such as sulfides,[21,22] selenide,[23,24] phosphides,[20,25] oxides,[26,27] and nitrides,[28,29,13] which showed great potential to replace the noble metals, and with the merits of low cost. However, there are still some urgent problems needed to be solved. Firstly, the current studies generally use simulated seawater instead of real seawater for the tests, while the effect of the complex environment of real seawater on the catalyst surface is avoided. Secondly, the electrocatalytic activity was only studied at a relatively low potential,[30] which is far from the requirement of the industrial application (over 500 mA cm^{-2}). Thirdly, the synthesized methods are usually complex and time-consuming, which covers a shadow on the industrial application of the prepared catalysts. Hence, it is urgently needed to explore a simple and highly efficient strategy to prepare the catalysts for seawater electrolysis with high performance and large current densities.

In this work, a one-step and rapid electrodeposition method to synthesize the P-Ni_4Mo/CF catalysts was proposed, which are highly efficient and durable for seawater electrolysis. P-Ni_4Mo/CF exhibited the current density of 100 mA cm^{-2} with an overpotential (η) of ~260 mV, which is very competitive, and only 88 mV away from commercial Pt/C catalyst (172 mV). In addition, the catalyst also displayed excellent stability, and no performance decay can be observed after a durability test for 200 h. Furthermore, the P-Ni_4Mo/CF reaches an impressive current density of 1.0 A cm^{-2} at an overpotential of 551 mV. It's proposed that the special nanoflower structure ensured abundant mass transfer channels and more active sites accessible, resulting in the high activity, and the performance was further enhanced with the P-doping. Our work not only develops a high-performance phosphorus-doped transition metal catalyst for seawater electrolysis, but also provides insights into the development of industry-standard, inexpensive catalysts.

n RESULTS AND DISCUSSION

The P-Ni_4Mo/CF catalyst was synthesized by a one-step electrodeposition method, as shown in Figure 1a. P-Ni_4Mo is grown directly on the CF and spatially interconnected to form many voids. X-ray diffraction (XRD) patterns display those three peaks located at 43.54°, 50.64°, and 74.30° are assigned to (211), (310), and (420) planes of P-Ni_4Mo, respectively. Compared to Ni_4Mo

DOI: 10.14102/j.cnki.0254-5861.2022-0110

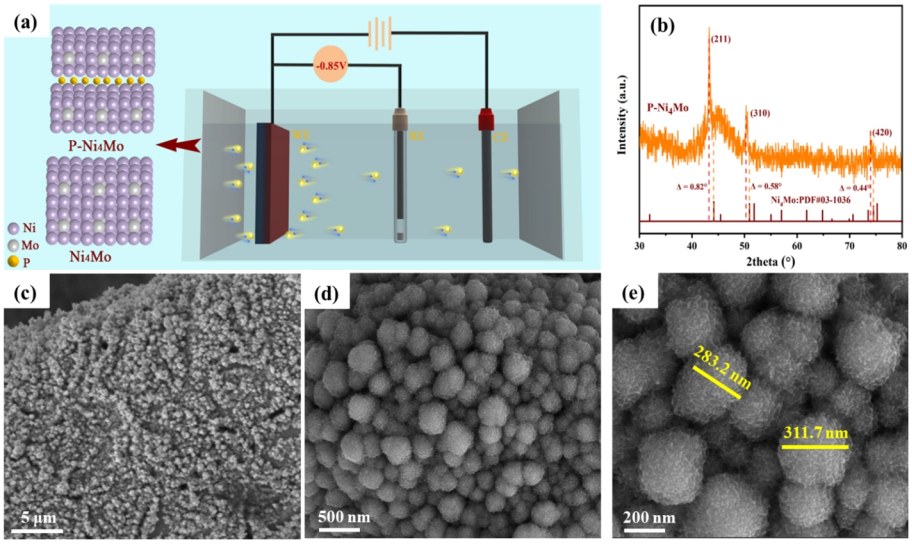

Figure 1. (a) Synthetic illustration of P-Ni_4Mo/CF. (b) XRD patterns of P-Ni_4Mo. (c-e) SEM image of P-Ni_4Mo/CF.

(PDF#03-1036), the P-Ni_4Mo shows a negative shift in the diffraction peaks, suggesting the successful P doping (Figure 1b). Figure 1c shows the uniform coverage of P-Ni_4Mo on the surface of CF. Figure 1d-e presents the formation of a nano-flower structure by catalyst P-Ni_4Mo/CF. This special structure has excellent catalytic activity specific surface area and abundant active material, which may facilitate the catalyst to fully contact the electrolyte and thus increase the reaction rate. Meanwhile, copper foam is a 3D porous material with excellent electrical conductivity and provides a large specific surface area favorable for electron transport, and the nano-flower structure of P-Ni_4Mo provides active and adsorption sites.

The transmission electron microscopy (TEM) image shows that P-Ni_4Mo is uniformly distributed in the copper network and appears as nanosheets (Figure 2b). An overlapping lamellar shape of the nanosheets is observed in the HRTEM image (Figure 2c), which is consistent with the SEM data (Figure 1c). Figure 2d displays the distinct lattice spacing of 2.07 Å, which is consistent with

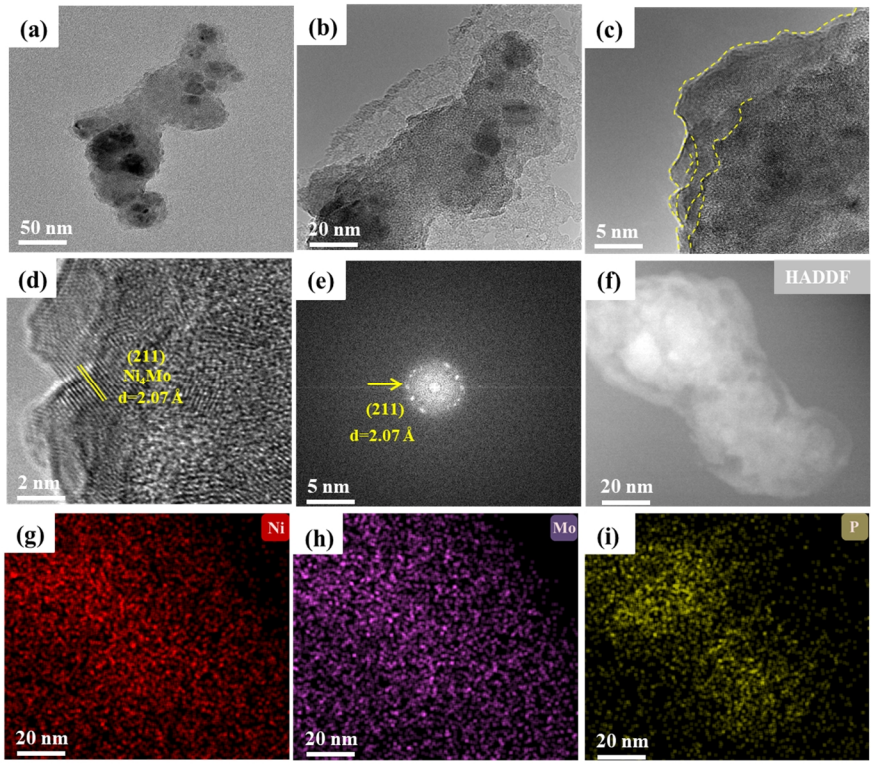

Figure 2. (a-d) The TEM image of P-Ni_4Mo. (e) SAED pattern. (f) HAADF image of P-Ni_4Mo and (g-i) the corresponding elemental mappings of Ni (red), Mo (purple) and P (yellow).

DOI: 10.14102/j.cnki.0254-5861.2022-0110

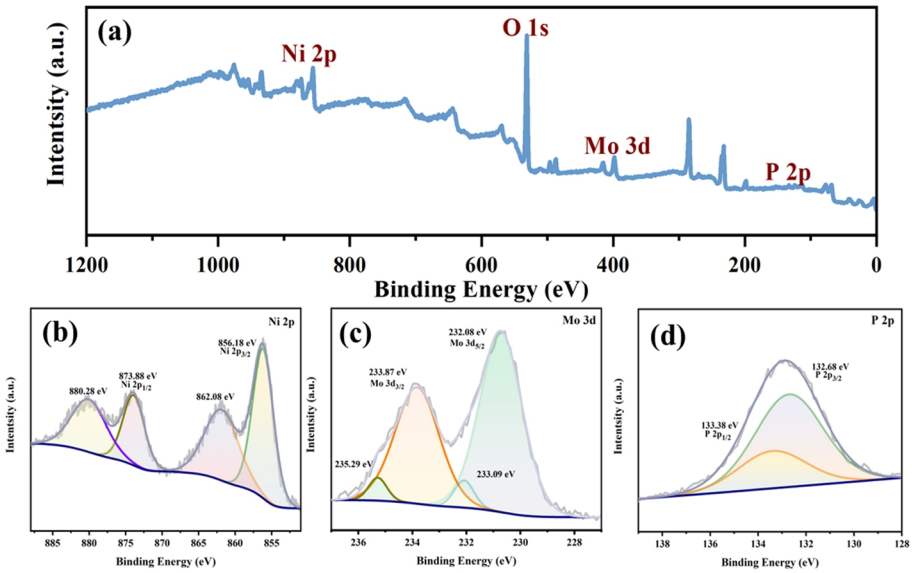

Figure 3. (a) XPS spectra of P-Ni_4Mo, and high-resolution of (b) Ni 2p, (c) Mo 3d, and (d) P 2p.

the (211) planar distance of Ni_4Mo (Figure 2e). High magnification HAADF-TEM and energy-dispersive X-ray spectroscopy (EDS) images show that Ni, Mo, and P are uniformly distributed across the P-Ni_4Mo (Figure 2f-i). The chemical states of P-Ni_4Mo are studied by XPS (Figure 3a), and Figure 3b displays four peaks located at 856.18, 862.08, 873.88, and 880.28 eV, respectively. The two peaks appearing at 856.18 and 873.88 eV are assigned to Ni $2p_{3/2}$ and Ni $2p_{1/2}$ binding energies of Ni_4Mo, and the other two peaks at 862.08 and 880.28 eV are related to satellite peaks, respectively.[31] Figure 2c shows that in the Mo 3d spectrum, the two peaks at Mo $3d_{5/2}$ (232.18 eV) and Mo $3d_{3/2}$ (235.28 eV) are attributed to the Ni_4Mo.[32] In addition, two small peaks at 232.08 and 235.29 eV are attributed to Mo^{6+}.[33] The peaks of P 2p are centered at 132.68 and 133.38 eV, which are attributed to M-P and P-O, respectively (Figure 3d).[34] Thus, this result combined with XRD and TEM confirms that P is successfully doped in the Ni_4Mo.

In a typical three-electrode system, P-Ni_4Mo/CF was used directly as a working electrode to evaluate the electrocatalytic activity of P-Ni_4Mo/CF for HER under 1.0 M KOH + seawater. For comparison, the catalytic activities of Pt/C, Ni_4Mo/CF and bare CF were also measured. It can be seen that P-Ni_4Mo/CF exhibited a significant catalytic activity towards HER (Figure 4a), which is much higher than that of Ni_4Mo/CF and CF. P-Ni_4Mo/CF produced a current density of 100 mA cm^{-2} at an overpotential (η) of 260 mV. In addition, the current density of 1.0 A cm^{-2} can reach an overpotential of 551 mV, which is close to that of a commercial Pt/C catalyst (453 mV). As shown in Figure 4b, P-Ni_4Mo/CF possessed a lower overpotential of 150, 260, and 422 mV than those of Ni_4Mo/CF catalysts at current densities of 10, 100, and 500 mA cm^{-2}, respectively, implying that phosphorus doping can greatly enhance the catalytic activity. Figure S5 shows the performance of HER under three different electrolytes, KOH + seawater, KOH + NaCl, and KOH systems, and compares it with the literature, as shown in Table S1, suggesting the activity of P-Ni_4Mo/CF is comparable or even better than that of the recently published papers. The Tafel slope of 90.6 mV dec^{-1} for P-Ni_4Mo/CF is slightly larger than that of Pt/C, while much lower than that of Ni_4Mo/CF (148.2 mV dec^{-1}) and CF (210.1 mV dec^{-1}), respectively, suggesting more favorable kinetics and higher catalytic activity of P-Ni_4Mo/CF catalyst (Figure 4c).

To better analyze the HER mechanism, the electrochemical impedance spectroscopy (EIS) was tested at an overpotential of 10 mA cm^{-2}, and the intrinsic properties of the prepared samples were evaluated (Figure 4d). The charge transfer resistance (R_{ct}) is related to the electrocatalytic kinetic properties of the electrolysis and catalyst interface. In general, smaller R_{ct} values indicated a faster electron transfer.[35] The R_{ct} of P-Ni_4Mo/CF (R_{ct} = 1.2 Ω) is much lower than that of Ni_4Mo/CF (R_{ct} = 3.6 Ω) and CF (R_{ct} = 11.4 Ω), which indicated that P doping enhanced the conductivity of Ni_4Mo/CF.[36] In addition, P-Ni_4Mo/CF, Ni_4Mo/CF, and CF all showed excellent conductivity, demonstrating excellent ion transfer between the electrode and electrolyte (Table S2).[37] The electrochemically active surface area (ECSA) of different catalysts was evaluated, which can reflect the number of electrocatalytic active sites.[38] The magnitude of (C_{dl}) can be determined by calculating the relationship between different scan rates and current density. As presented in Figure 4e, P-Ni_4Mo/CF showed a slope value of 45.9 mF cm^{-2}, which is remarkably larger than that of Ni_4Mo/CF (32.4 mF cm^{-2}), suggesting the introduction of P can increase the number of active sites and the catalytic activity. The actual versus theoretical hydrogen production of the P-Ni_4Mo/CF catalyst was measured at the current density of 100 mA cm^{-2} for 108 min (Figure 4f). P-Ni_4Mo/CF gave a Faraday efficiency of ~99.1% in the HER process, demonstrating its excellent conversion efficiency. The Multi-order potential stability test was performed, and the test curve remained smooth at each stage as the current density increased from 10 to 50 mA cm^{-2}, indicating that P-Ni_4Mo/CF has good stability, conductivity, and excellent electron transfer capability (Figure 4g, green line). To evaluate the long-term stability of P-Ni_4Mo/CF, current density versus time (i-t) curves were recorded. P-Ni_4Mo/CF maintained its catalytic acti-

Chin. J. Struct. Chem. **2022**, 41, 2207068-2207073
DOI: 10.14102/j.cnki.0254-5861.2022-0110

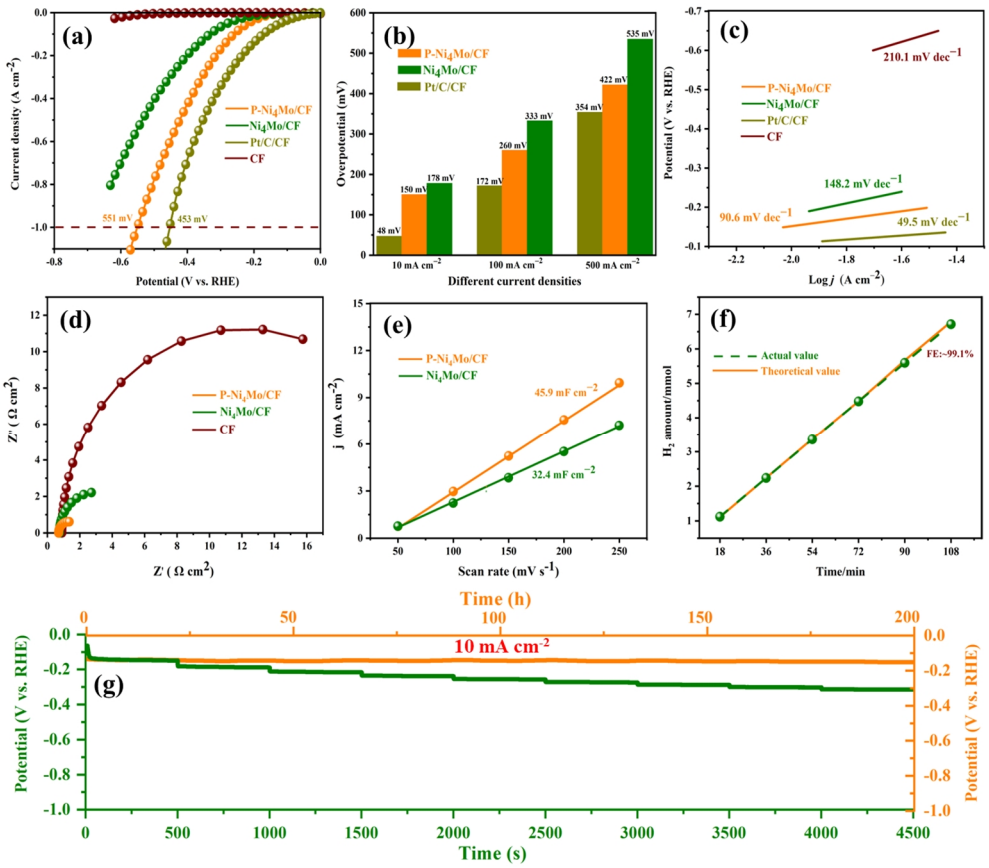

Figure 4. (a) LSV curves of different materials. (b) Overpotential corresponding to different current densities. (c) Corresponding Tafel plots with linear fitting. (d) The estimation of C_{dl}. (e) EIS spectra were measured at 10 mA cm^{-2}. (f) Electrocatalysts efficiency of P-Ni$_4$Mo/CF for HER. (g) Multipotential stability test of P-Ni$_4$Mo/CF and long-term constant current stability test P-Ni$_4$Mo/CF at 10 mA cm^{-2}.

vity after a durability test at 10 mA cm^{-2} for 200 h (Figure 4g, yellow line), which is much better than many recently published literatures, such as Ni-SA/NC only for 14 h,[39] Ru-CoO$_x$/NF for 100 h,[40] and Ni-SN@C for 40 h,[28] demonstrating the high durability of P-Ni$_4$Mo/CF catalyst.[41]

The overall morphology of P-Ni$_4$Mo/CF after durability test was examined by SEM, and no big differences can be observed compared with the initial materials, suggesting the structural stability of the catalyst (Figure S3). XPS measurements were also performed after the durability test. Figure S4a shows the XPS of Ni, and two peaks centered at Ni 2p$_{3/2}$ (855.68 eV) and Ni 2p$_{1/2}$ (873.17 eV), respectively, corresponding to Ni(OH)$_2$,[42] and the other two satellites peaks (861.48 and 879.67 eV) are related to NiO.[43] For Mo 3d, two obvious peaks centered at 231.88 and 234.67 eV are attributed to the oxidation state of Mo, Mo^{5+} (Figure S4b).[44,45] For P 2p, the characteristic peaks located at 133.38 and 134.98 eV belong to PO_4^{3-} (Figure S4c).[46] For O 1s (Figure S4d), three peaks located at 530.57, 530.98, and 532.58 eV are respectively attributed to M-O, OH^- and H_2O.[47-49] Therefore, the catalyst undergoes surface reconstruction to form metal oxidate after the long-term stability, while the HER performance is still well preserved.

n CONCLUSIONS

In summary, P-Ni$_4$Mo/CF catalysts were successfully prepared by a rapid one-step electrodeposition method, and were applied for the electrolysis of seawater. The overpotential at 100 mA cm^{-2} is only 260 mV, and the current density can reach up to 1.0 A cm^{-2} at the overpotential of 551 mV. P-Ni$_4$Mo/CF also exhibits significant HER stability and can be stably operated for 200 h. The excellent HER activity of the obtained P-Ni$_4$Mo/CF can be attributed to the high conductivity of the catalyst, the high specific surface area, and the electronic structure modulation due to the P doping. Our research may provide a new avenue for the development of cost-effective, highly stable and active catalysts for seawater electrolysis.

n ACKNOWLEDGEMENTS

This work was supported by the Natural Science Foundation of Hainan Province (221RC1018), the National Natural Science Foundation of China (22109034, 22109035, 52164028, 62105083), the Opening Project of Key Laboratory of Electrochemical Energy Storage and Energy Conversion of Hainan Province (KFKT2021007), and the Foundation of State Key Laboratory of Marine Resource Utilization in South China Sea (Hainan University, Grant No. MRUKF2021029).

n AUTHOR INFORMATION

DOI: 10.14102/j.cnki.0254-5861.2022-0110

Corresponding authors. Emails: jli@hainanu.edu.cn (J. Li) and 521000hua282@sina.com (Y. Hua)

n COMPETING INTERESTS

The authors declare no competing interests.

n ADDITIONAL INFORMATION

Supplementary information is available for this paper at http://manu30.magtech.com.cn/jghx/EN/10.14102/j.cnki.0254-5861.2022-0110

For submission: https://mc03.manuscriptcentral.com/cjsc

n REFERENCES

(1) Tian, X.; Zhao, X.; Su, Y.-Q.; Wang, L.; Wang, H.; Dang, D.; Chi, B.; Liu, H.; Hensen, E. J.; Lou, X. W. Engineering bunched Pt-Ni alloy nanocages for efficient oxygen reduction in practical fuel cells. *Science* **2019**, 366, 850-856.

(2) Liu, Z.; Zeng, L.; Yu, J.; Yang, L.; Zhang, J.; Zhang, X.; Han, F.; Zhao, L.; Li, X.; Liu, H. Charge redistribution of Ru nanoclusters on Co_3O_4 porous nanowire via the oxygen regulation for enhanced hydrogen evolution reaction. *Nano Energy* **2021**, 85, 105940.

(3) Feng, S.; Luo, J.; Li, J.; Yu, Y.; Kang, Z.; Huang, W.; Chen, Q.; Deng, P.; Shen, Y.; Tian, X. Heterogeneous structured Ni_3Se_2/MoO_2@$Ni_{12}P_5$ catalyst for durable urea oxidation reaction. *Mater. Today Phys.* **2022**, 23, 100646.

(4) Yang, Y.; Wu, D.; Yu, Y.; Li, J.; Rao, P.; Jia, C.; Liu, Z.; Chen, Q.; Huang, W.; Luo, J.; Deng, P.; Shen, Y.; Tian, X. Bridge the activity and durability of ruthenium for hydrogen evolution reaction with the RuOC link. *Chem. Eng. J.* **2022**, 433, 134421.

(5) Yu, Y.; Chen, Q.; Li, J.; Rao, P.; Li, R.; Du, Y.; Jia, C.; Huang, W.; Luo, J.; Deng, P.; Shen, Y.; Tian, X. Progress in the development of heteroatom-doped nickel phosphates for electrocatalytic water splitting. *J. Colloid Interface Sci.* **2022**, 607, 1091-1102.

(6) Zheng, X.; Wu, D.; Liu, Y.; Li, J.; Yang, Y.; Huang, W.; Liu, W.; Shen, Y.; Tian, X. Photocatalytic reduction of water to hydrogen by $CuPbSbS_3$ nanoflakes. *Mater. Today Energy* **2022**, 25, 100956.

(7) Gao, M.; Zhou, W.-Y.; Mo, Y.-X.; Sheng, T.; Deng, Y.; Chen, L.; Wang, K.; Tan, Y.; Zhou, H. Outstanding long-cycling lithium-sulfur batteries by core-shell structure of S@Pt composite with ultrahigh sulfur content. *Adv. Powder Mater.* **2022**, 1, 100006.

(8) Li, Z.; Wu, X.; Jiang, X.; Shen, B.; Teng, Z.; Sun, D.; Fu, G.; Tang, Y. Surface carbon layer controllable Ni_3Fe particles confined in hierarchical N-doped carbon framework boosting oxygen evolution reaction. *Adv. Powder Mater.* **2021**, 1, 100020.

(9) Li, P. Y.; Hong W. T.; Liu, W. Fabrication of large scale self-supported WC/$Ni(OH)_2$ electrode for high-current-density hydrogen evolution. *Chin. J. Struct. Chem.* **2021**, 40, 1365-1371.

(10) Yang, Y.; Yu, Y.; Li, J.; Chen, Q.; Du, Y.; Rao, P.; Li, R.; Jia, C.; Kang, Z.; Deng, P. Engineering ruthenium-based electrocatalysts for effective hydrogen evolution reaction. *Nano-Micro. Lett.* **2021**, 13, 1-20.

(11) Rao, P.; Luo, J.; Li, J.; Huang, W.; Sun, W.; Chen, Q.; Jia, C.; Liu, Z.; Deng, P.; Shen, Y.; Tian, X. One-dimensional PtFe hollow nanochains for the efficient oxygen reduction reaction. *Carbon Energy* **2022**, https://doi.org/10.1002/cey2.192

(12) Wu, Y. L.; Xie, N.; Li, X. F.; Fu, Z. M.; Wu, X. T.; Zhu Q. L. MOF-derived hierarchical hollow NiRu-C nanohybrid for efficient hydrogen evolution reaction. *Chin. J. Struct. Chem.* **2021**, 40, 1346-1356.

(13) Yu, L.; Zhu, Q.; Song, S.; McElhenny, B.; Wang, D.; Wu, C.; Qin, Z.; Bao, J.; Yu, Y.; Chen, S. Non-noble metal-nitride based electrocatalysts for high-performance alkaline seawater electrolysis. *Nat. Commun.* **2019**, 10, 1-10.

(14) Deng, Y.; Luo, J.; Chi, B.; Tang, H.; Li, J.; Qiao, X.; Shen, Y.; Yang, Y.; Jia, C.; Rao, P.; Liao, S.; Tian, X. Advanced atomically dispersed metal-nitrogen-carbon catalysts toward cathodic oxygen reduction in PEM fuel cells. *Adv. Energy Mater.* **2021**, 11, 2101222.

(15) Rao, P.; Wang, T.-J.; Li, J.; Deng, P.; Shen, Y.; Chen, Y.; Tian, X. Plasma induced Fe-N active sites to improve the oxygen reduction reaction performance. *Adv. Sens. Energy Mater.* **2022**, 1, 100005.

(16) Rao, P.; Wu, D.; Luo, J.; Li, J.; Deng, P.; Shen, Y.; Tian, X. A plasma bombing strategy to synthesize high-loading single-atom catalysts for oxygen reduction reaction. *Cell Rep. Phys. Sci.* **2022**, 3, 100880.

(17) Tian, H.; Wu, D.; Li, J.; Luo, J.; Jia, C.; Liu, Z.; Huang, W.; Chen, Q.; Shim, C. M.; Deng, P.; Shen, Y.; Tian, X. Rational design ternary platinum based electrocatalysts for effective methanol oxidation reaction. *J. Energy Chem.* **2022**, 70, 230-235.

(18) Dresp, S. R.; Dionigi, F.; Klingenhof, M.; Strasser, P. Direct electrolytic splitting of seawater: opportunities and challenges. *ACS Energy Lett.* **2019**, 4, 933-942.

(19) Wu, H. S.; Miao, T. F.; Shi, H. X.; Xu, Y.; Fu, X. L.; Qian, L. Probing photocatalytic hydrogen evolution of cobalt complexes: experimental and theoretical methods. *Chin. J. Struct. Chem.* **2021**, 40, 1696-1709.

(20) Ma, Y.-Y.; Wu, C.-X.; Feng, X.-J.; Tan, H.-Q.; Yan, L.-K.; Liu, Y.; Kang, Z.-H.; Wang, E.-B.; Li, Y.-G. Highly efficient hydrogen evolution from seawater by a low-cost and stable CoMoP@C electrocatalyst superior to Pt/C. *Energy Environ. Sci.* **2017**, 10, 788-798.

(21) Wang, C.; Zhu, M.; Cao, Z.; Zhu, P.; Cao, Y.; Xu, X.; Xu, C.; Yin, Z. Heterogeneous bimetallic sulfides based seawater electrolysis towards stable industrial-level large current density. *Appl. Catal., B* **2021**, 291, 120071.

(22) Yu, L.; Wu, L.; McElhenny, B.; Song, S.; Luo, D.; Zhang, F.; Yu, Y.; Chen, S.; Ren, Z. Ultrafast room-temperature synthesis of porous S-doped Ni/Fe (oxy) hydroxide electrodes for oxygen evolution catalysis in seawater splitting. *Energy Environ. Sci.* **2020**, 13, 3439-3446.

(23) Chang, J.; Wang, G.; Yang, Z.; Li, B.; Wang, Q.; Kuliiev, R.; Orlovskaya, N.; Gu, M.; Du, Y.; Wang, G. Dual-doping and synergism toward high-performance seawater electrolysis. *Adv. Mater.* **2021**, 33, 2101425.

(24) Yang, C.; Zhou, L.; Wang, C.; Duan, W.; Zhang, L.; Zhang, F.; Zhang, J.; Zhen, Y.; Gao, L.; Fu, F. Large-scale synthetic Mo@(2H-1T)-$MoSe_2$ monolithic electrode for efficient hydrogen evolution in all pH scale ranges and seawater. *Appl. Catal., B* **2022**, 304, 120993.

(25) Wu, L. B.; Yu, L.; McElhenny, B.; Xing, X. X.; Luo, D.; Zhang, F. H.; Bao, J. M.; Chen, S.; Ren, Z. F. Rational design of core-shell-structured CoP_x@FeOOH for efficient seawater electrolysis. *Appl. Catal. B-Environ.* **2021**, 294, 120256.

(26) Tran, P. K. L.; Tran, D. T.; Malhotra, D.; Prabhakaran, S.; Kim, D. H.; Kim, N. H.; Lee, J. H. Highly effective freshwater and seawater electrolysis enabled by atomic Rh-modulated Co-CoO lateral heterostructures. *Small* **2021**, 17, 2103826.

(27) ul Haq, T.; Haik, Y. S doped Cu_2O-CuO nanoneedles array: free standing oxygen evolution electrode with high efficiency and corrosion resistance for seawater splitting. *Catal. Today* **2021**, 17, 0920-5861.

DOI: 10.14102/j.cnki.0254-5861.2022-0110

(28) Jin, H.; Wang, X.; Tang, C.; Vasileff, A.; Li, L.; Slattery, A.; Qiao, S. Z. Stable and highly efficient hydrogen evolution from seawater enabled by an unsaturated nickel surface nitride. *Adv. Mater.* **2021**, 33, 2007508.
(29) Yu, L.; Wu, L.; Song, S.; McElhenny, B.; Zhang, F.; Chen, S.; Ren, Z. Hydrogen generation from seawater electrolysis over a sandwich-like NiCoN|Ni_xP|NiCoN microsheet array catalyst. *ACS Energy Lett.* **2020**, 5, 2681-2689.
(30) Liang, C.; Zou, P.; Nairan, A.; Zhang, Y.; Liu, J.; Liu, K.; Hu, S.; Kang, F.; Fan, H. J.; Yang, C. Exceptional performance of hierarchical Ni-Fe oxyhydroxide@NiFe alloy nanowire array electrocatalysts for large current density water splitting. *Energy Environ. Sci.* **2020**, 13, 86-95.
(31) Londoño-Calderón, V.; Ospina, R.; Rodriguez-Pereira, J.; Rincón-Ortiz, S. A.; Restrepo-Parra, E. Molybdenum and nickel nanoparticles synthesis by laser ablation towards the preparation of a hydrodesulfurization catalyst. *Catalysts* **2020**, 10, 1076.
(32) Du, W.; Shi, Y.; Zhou, W.; Yu, Y.; Zhang, B. Unveiling the in situ dissolution and polymerization of Mo in Ni_4Mo alloy for promoting the hydrogen evolution reaction. *Angew. Chem. Int. Ed.* **2021**, 60, 7051-7055.
(33) Jin, Z.; Wang, L.; Chen, T.; Liang, J.; Zhang, Q.; Peng, W.; Li, Y.; Zhang, F.; Fan, X. Transition metal/metal oxide interface (Ni-Mo-O/Ni_4Mo) stabilized on N-doped carbon paper for enhanced hydrogen evolution reaction in alkaline conditions. *Ind. Eng. Chem. Res.* **2021**, 60, 5145-5150.
(34) Hao, Y.; Du, G.; Fan, Y.; Jia, L.; Han, D.; Zhao, W.; Su, Q.; Ding, S.; Xu, B. Mo/P dual-doped co/oxygen-deficient Co_3O_4 core-shell nanorods supported on Ni foam for electrochemical overall water splitting. *ACS Appl. Mater. Interfaces* **2021**, 13, 55263-55271.
(35) Huang, S.; Ouyang, T.; Zheng, B. F.; Dan, M.; Liu, Z. Q. Enhanced photoelectrocatalytic activities for CH_3OH-to-HCHO conversion on Fe_2O_3/MoO_3: Fe-O-Mo covalency dominates the intrinsic activity. *Angew. Chem. Int. Ed.* **2021**, 60, 9546-9552.
(36) Wang, X.; Wang, J.; Yu, B.; Jiang, W.; Wei, J.; Chen, B.; Xu, R.; Yang, L. Facile synthesis $MnCo_2O_{4.5}$@C nanospheres modifying PbO_2 energy-saving electrode for zinc electrowinning. *J. Hazard. Mater.* **2022**, 428, 128212.
(37) Lee, J.; Jung, H.; Park, Y. S.; Woo, S.; Yang, J.; Jang, M. J.; Jeong, J.; Kwon, N.; Lim, B.; Han, J. W. High-efficiency anion-exchange membrane water electrolyzer enabled by ternary layered double hydroxide anode. *Small* **2021**, 17, 2100639.
(38) Xue, S.; Wu, G.; Li, M.; Liu, Z.; Deng, Y.; Han, W.; Lv, X.; Wan, S.; Xi, X.; Yang, D. Generalized assembly of sandwich-like 0D/2D/0D heterostructures with highly exposed surfaces toward superior electrochemical performances. *Nano Res.* **2022**, 15, 255-263.
(39) Zang, W.; Sun, T.; Yang, T.; Xi, S.; Waqar, M.; Kou, Z.; Lyu, Z.; Feng, Y. P.; Wang, J.; Pennycook, S. J. Efficient hydrogen evolution of oxidized Ni-N_3 defective sites for alkaline freshwater and seawater electrolysis. *Adv. Mater.* **2021**, 33, 2003846.
(40) Wu, D.; Chen, D.; Zhu, J.; Mu, S. Ultralow Ru Incorporated amorphous cobalt-based oxides for high-current-density overall water splitting in alkaline and seawater media. *Small* **2021**, 17, 2102777.
(41) Zheng, B.-F.; Ouyang, T.; Wang, Z.; Long, J.; Chen, Y.; Liu, Z.-Q. Enhanced plasmon-driven photoelectrocatalytic methanol oxidation on Au decorated α-Fe_2O_3 nanotube arrays. *Chem. Commun.* **2018**, 54, 9583-9586.
(42) Tao, S.; Wen, Q.; Jaegermann, W.; Kaiser, B. Formation of highly active NiO(OH) thin films from electrochemically deposited $Ni(OH)_2$ by a simple thermal treatment at a moderate temperature: a combined electrochemical and surface science investigation. *ACS Catal.* **2022**, 12, 1508-1519.
(43) Wang, F.; Sun, X.; Wang, Y.; Zhou, H.; Yin, J.; Zhang, X. Metallized $Ni(OH)_2$·NiO/FeOOH on Ni foam as a highly effective water oxidation catalyst prepared by surface treatment: oxidation-corrosion equilibrium. *ACS Appl. Energy Mater.* **2021**, 4, 5599-5605.
(44) Lu, Q.; Huang, B.; Zhang, Q.; Chen, S.; Gu, L.; Song, L.; Yang, Y.; Wang, X. Single-crystal inorganic helical architectures induced by asymmetrical defects in sub-nanometric wires. *J. Am. Chem. Soc.* **2021**, 143, 9858-9865.
(45) Wang, M.; Ye, C.; Xu, M.; Bao, S. MoP nanoparticles with a P-rich outermost atomic layer embedded in N-doped porous carbon nanofibers: self-supported electrodes for efficient hydrogen generation. *Nano Res.* **2018**, 11, 4728-4734.
(46) Yu, C.; Xu, F.; Luo, L.; Abbo, H. S.; Titinchi, S. J.; Shen, P. K.; Tsiakaras, P.; Yin, S. Bimetallic Ni-Co phosphide nanosheets self-supported on nickel foam as high-performance electrocatalyst for hydrogen evolution reaction. *Electrochim. Acta* **2019**, 317, 191-198.
(47) Panigrahi, K.; Howli, P.; Chattopadhyay, K. K. Three-dimensional VO_2@PANI micro flower array for flexible supercapacitor. *Mater. Lett.* **2019**, 253, 90-94.
(48) She, X.; Liu, L.; Ji, H.; Mo, Z.; Li, Y.; Huang, L.; Du, D.; Xu, H.; Li, H. Template-free synthesis of 2D porous ultrathin nonmetal-doped g-C_3N_4 nanosheets with highly efficient photocatalytic H_2 evolution from water under visible light. *Appl. Catal., B* **2016**, 187, 144-153.
(49) Wang, S.; Lu, Z.; Fang, Y.; Zheng, T.; Zhang, Z.; Wang, W.; Zhao, R.; Xue, W. Controllable synthesis of self-templated hierarchical Ni_3S_2@N-doped carbon for enhanced oxygen evolution reaction. *Mater. Adv.* **2021**, 2, 3971-3980.

Received: May 7, 2022
Accepted: May 30, 2022
Published online: June 8, 2022
Published: July 18, 2022

DOI: 10.14102/j.cnki.0254-5861.2022-0110